Supporting Information

Devignes et al. 10.1073/pnas.1718009115

SI Methods

Mice. All animal protocols were reviewed and approved by the Institutional Animal Care and Use Committee of the University of California, San Francisco and the French National Animal Ethic Committee, CEEA9. Floxed *Vhlh*, floxed *Hif1α*, floxed *Hif2α*, and Osx-Cre::GFP mice and genotyping protocols are described elsewhere (1–4). All mice were backcrossed into FVB/n wild-type mice for at least 10 generations. Littermate mice carrying either one copy of the Osx-Cre::GFP transgene without the floxed allele or negative for the Osx-Cre::GFP transgene were used equally as control animals. They were phenotypically indistinguishable and gave identical results in our study. Control and mutant animals were maintained on a high-fat diet supplemented with easily accessible DietGel food (72015022; Bio Services) after weaning.

Cell Lines. Two BCC lines were generated from late mammary carcinomas obtained from two independent MMTV-PyMT transgenic mice (5) that express the PyMT oncoprotein under the control of MMTV LTR on the pure FVB/n background. Both lines gave similar results in our in vivo experiments; data obtained with BCC line 1 are shown. These cell lines are negative for ER and PR and produce osteolytic bone metastases (Fig. S2). The reporter genes encoding luciferase (pMSCVpuro-Luc) and GFP (pMIG-GFP) were inserted in BCC to evaluate tumor growth and dissemination in live animals. The resulting cell line, BCC-GFP::LUC, has been tested and authenticated for morphology by microscopic observation of a typical transformed mesenchymal-like phenotype and for growth by passaging cells at a fixed frequency and dilution to detect any drift in the proliferation rate of the cells. Species and genetic background were verified by transplanting breast cancer cells into FVB/n immunocompetent recipient mice; and mycoplasma contamination was tested and found negative using DAPI staining and PCR for mycoplasma DNA. (Primer pairs: ACACCATGGGAGCTGGTAAT; CTTCATCGACTTTCAGATCCCAAGGCAT and GTTCTTTGAAAACTGAAT; GCATCCACCAAAAACTCT). BCC-GFP::LUC, NT2.5 (6), and 4T1 cells were maintained in DMEM supplemented with 10% FBS, and 5 μg/mL puromycin. The calvarial immature osteoblast cell line MC3T3 was maintained in αMEM with 10% FBS and 2 mM L-glutamine. The osteocyte-like cell line MLO-Y4 was maintained in αMEM with 5% FBS, 5% calf serum, and 2 mM L-glutamine.

Primary Cell Culture. Chondrocytes were isolated from collagenase-digested articular cartilage from 5-d-old mice and were cultured in DMEM supplemented with 10% FBS and 2 mM L-glutamine. Bone marrow was obtained by flushing long bones from 5-wk-old mice. MSPCs were isolated as previously described (7) from crushed long bones (epiphyses and marrow were removed) of 5-wk-old control, $\Delta Hif1\alpha^{OSX}$, and $\Delta Vhlh^{OSX}$ mice. Cells that migrated out of bone chips were cultured in αMEM with 10% FBS and 2 mM L-glutamine and were used after the third passage. We verified that cells expressed skeletal progenitor markers by qPCR and that they were able to differentiate into chondrocytes, osteoblasts, and to (a lesser extent) adipocytes. For all experiments 10^4 cells/cm^2 were plated. Bone explants (crushed long bones washed to eliminate bone marrow cells) of 5-wk-old mice were maintained in αMEM with 0.25% FBS and 2 mM L-glutamine.

Transduction, siRNA, and Cocultures. The BCC-CTL and BCC-shCXCR4 lines were obtained by infecting the cells with lentiviral particles encoding GFP or shCXCR4-GFP (8). Mixtures of four control siRNAs and of four siRNAs against *Cxcl12* were purchased from Dharmacon. MSPCs were transfected using Lipofectamine RNAiMax (Invitrogen) with siRNA at a final concentration of 25 nM. Migration assays were performed overnight by seeding 5,000 BCC-GFP::LUC cells on cell-culture inserts with an 8-μm pore size and placing them above serum-starved MSPCs, above an empty well with serum-free medium as control, or above medium supplemented with 10% FBS or with murine recombinant CXCL12 (100 μg/mL; PeproTech). Insert membranes were then scrubbed to remove nonmigrating cells, fixed in methanol, and mounted in mounting medium with DAPI (Vector Laboratories). The number of cells/mm^2 was then quantified on the whole insert membrane. Proliferation assays were performed by incubating serum-starved BCC-GFP::LUC cells for 24 h with the supernatant of serum-starved MSPCs, serum-free medium as negative control, or medium supplemented with 10% FBS or with murine recombinant CXCL12 (100 μg/mL; PeproTech). MTT (Sigma) was then added at 0.3 mg/mL and incubated for 1 h at 37 °C. MTT was solubilized with DMSO and OD 550 nm was measured. In both assays, the CXCR4 inhibitor AMD3100 (25 μg/mL; Sigma) or vehicle (saline) was preincubated for 30 min.

Breast Cancer Cell Inoculation. Methods for i.c. injection, i.v. (tail vein) injection, and orthotopic i.f.p. transplantation are described elsewhere (9, 10). Breast cancer cells were inoculated in syngeneic 8-wk-old control and mutant FVB/n mice. Male and female mutant mice gave identical results in terms of bone and lung metastasis and were equally used for i.c. and i.v. injections. Only females were used for i.f.p. transplantation. For i.c. injections, 10^5 BCC-GFP::LUC cells in 50 μL HBSS were injected into the left ventricle for the experiments presented in Figs. 1–3; 10^4 BCC-GFP::LUC were used for i.c. experiments in Fig. 6 and Figs. S4 and S5. For i.v. injection, 5×10^5 BCC-GFP::LUC cells in 200 μL HBSS were injected into the tail vein. For i.f.p. transplantation, mice were injected into the fourth right mammary gland with 10^4 BCC-GFP::LUC cells in 50 μL of 50% Matrigel (354234; Corning) in HBSS, except for the $\Delta Hif1\alpha^{OSX}$ experiment, in which 10^5 BCC-GFP::LUC cells were used (Fig. 3 *A* and *B*). Tumor growth and dissemination were monitored longitudinally in live animals every 2–3 d by bioluminescence imaging, using D-Luciferin injections (Perkin-Elmer), following the manufacturer's instructions. Image acquisition was performed with the IVIS Lumina II imager (Perkin-Elmer) (Figs. 2 *C* and *E*, and 3 *A*, *C*, *K*, and *L*), the IVIS Spectrum imager (Perkin-Elmer) (Fig. 3 *G*–*J* and 6 *E* and *F* and Fig. S5*F*), or the ONYX dark box system (Stanford Photonics, Inc.) (Figs. 3 *M* and *N* and 6 *B*, *C*, *H*, *J*, and *K* and Figs. S1, S3, S4, and S5 *A*–*C*). Mice presenting a signal in the limbs for three consecutive imaging sessions were scored as positive on the first day of detection. The presence of bone metastases was then confirmed on histological sections. For histological detection of bone metastasis after i.f.p. injections, mice were scored positive if breast cancer cells were detected on hind limb sections, regardless of tumor size and number.

Drug Treatments. Drugs were administered s.c. 2 d before BCC-GFP::LUC inoculation and for the duration of the experiments. AMD3100 (A5602; Sigma) was injected daily at 1.25 mg/kg in saline. ALN (126855; Calbiochem) was injected once a week at 5 mg/kg.

Histological Analyses. Undecalcified bones were fixed in ethanol, dehydrated, and embedded in resin (methyl methacrylate) for histomorphometric analyses, as previously described (11). For paraffin or frozen-tissue processing, tissue samples were fixed in 4% paraformaldehyde overnight at 4 °C and then were decalcified in 20% EDTA (pH 7.4) at 4 °C with constant shaking for 10 d or 72 h, respectively, with three changes of solution changing. For immunofluorescence analyses, bones were frozen in 20% sucrose/2% polyvinylpyrrolidone (Sigma) as previously described (12), and 16-μm-thick frozen bone sections were obtained on a Leica cryostat. Bones embedded in paraffin were sectioned at 5 μm using a Leica microtome. Breast tumors were embedded in OCT compound and sectioned at 12 μm. Sections were stained with H&E and Safranin O.

Micro-CT and Histomorphometry. Micro-CT imaging and analyses were performed with a SkyScan 1172 (Bruker microCT), using a voxel size of 5.92 μm, a voltage of 69 kV, intensity of 100 μA, and exposure of 300 ms. NRecon reconstruction and DataViewer software was used for 3D reconstruction and analyses. Analysis of structural parameters for Fig. S4 was performed using CTAn and CTVox (Bruker microCT). Bone histomorphometry was done on resin sections as previously described (11). Eight-week-old female mice were used for all analyses except those in Fig. 4*A*, where 12-wk-old females were used. Aniline blue staining was performed to assess BV/TV and other structural parameters. Tartrate-resistant acid phosphatase (TRAP) staining was performed using naphthol ASTR phosphate (Sigma) as substrate. Sections were counterstained with methyl green, and $TRAP^+$ osteoclasts were expressed as the number of $TRAP^+$ cells per area of tissue or as a percentage of bone surface. Osteoid surface and osteoblast numbers were quantified by histomorphometry on femur sections stained for 15 min with a 1% Toluidine blue (pH 4.3) solution. A light blue staining reveals unmineralized matrix (osteoid). Results are expressed as the percentage of osteoid surface per bone surface and as the number of osteoblasts per area of bone surface for $\Delta Hif1\alpha^{OSX}$ mice. Osteoblast numbers were quantified by flow cytometry for $\Delta Vhlh^{OSX}$ mice because the structure of the bone is too altered in these mice to assess these numbers accurately. Two independent investigators blinded to genotypes analyzed all sections.

Immunohistochemistry. Specific antigen retrieval was applied when needed, as indicated in Table S1. Sections were blocked with TNB blocking buffer (FP1020; PerkinElmer) for 1 h at room temperature and then were incubated with primary antibody overnight at 4 °C. For immunofluorescent detection, sections were incubated at room temperature for 1 h with secondary antibodies diluted 1:100: donkey anti-rabbit IgG DyLight 550 conjugate, DyLight 480 conjugate, or donkey anti-rat IgG Dylight 650 conjugate (Pierce), except for anti-GFP antibody, for which no secondary antibody was needed. Nuclei were counterstained with DAPI at 0.1 μg/mL (Life Technologies). For chromogenic detection, ImmPRESS HRP polymer detection kit anti-rat and anti-rabbit (Vector Laboratories) were used, and color development was carried out using 3,3′-diaminobenzidine-tetrahydrochloride HRP substrate (Vector Labs). Sections were counterstained with Mayer's hematoxylin for 5 s. Hypoxyprobe (HP-500 mg; Hypoxyprobe Inc.) was injected at 60 mg/kg 4 h before mice were killed and tissue was collected. Dylight 549-conjugated antibody (HP7-1000Kit; Hypoxyprobe, Inc.) was used for detecting Hypoxyprobe on sections.

ELISA. Plasma samples from 8-wk-old mice were collected by cardiac puncture with an EDTA-coated syringe and were centrifuged for 15 min at 1,000 × *g* at 4 °C. The supernatant was collected and centrifuged for an additional 10 min at 10,000 × *g* at 4 °C. The Mouse VEGF Quantikine ELISA Kit and Mouse CXCL12/SDF-1 alpha Quantikine ELISA Kit (MMV00 and MCX120; R&D Systems) were used.

Flow Cytometry. Osteoblast-lineage cells were identified as Lin^-/$CD45^-$/$CD31^-$/$CD51^+$/$Sca\text{-}1^-$ cells from collagenase-digested bone chips from crushed bones of 5-wk-old control and mutant mice. as previously described (13). The presence of $Osx\text{-}GFP^+$ OPCs was examined in single-cell suspensions of bone marrow and spleen obtained from 5-wk-old Osx-Cre::GFP hemizygous mice stained for CD45 and hematopoietic lineage markers, as previously described (13). Cells were analyzed on a LSR II flow cytometer (BD Biosciences).

Western Blot Analysis. BCC-GFP::LUC cells were lysed in buffer (20 mM Tris, 150 mM NaCl, 1 mM EDTA, 1 mM EGTA, 1% Triton X-100, 2.5 mM sodium pyrophosphate, 1 mM β-glycerophosphate) with protease inhibitors (Sigma) and 1 mM orthovanadate. Lysates were separated by SDS/PAGE and transferred to nitrocellulose membranes, blocked with 5% milk for 1 h, and incubated with the following primary antibodies overnight at 4 °C: anti-phospho ERK1/2 and anti-ERK1/2 (1:2,000 and 1:500, respectively; 4370 and 4695; Cell Signaling) and anti–α-tubulin (1:1,000; Santa Cruz).

RNA Extraction, Reverse Transcription, and RT-qPCR. Tissues were crushed using a mortar and pestle. For tissues or cells, RNA was extracted using TRIzol reagent (Invitrogen) and the ISOLATE II RNA kit (Bioline). Reverse transcription was performed with random primers using the High-Capacity cDNA Reverse Transcription Kit (Applied Biosystems). Real-time qPCR was then performed using the primers listed below and the SensiFAST SYBR No-ROX Kit (Bioline) on a LightCycler 480 system (Roche). Primers were designed to overlap exon junctions using Primer3. Eukaryotic translation elongation factor 1 alpha 1 (*Eef1α*) was used as the housekeeping gene.

Eef1α: AGGTGATTATCCTGAACCATCC, TGCCAGGGACCATATCAACA;

Cxcr4: GGAACCGATCAGTGTGAGTATAT, AAGTAGATGGTGGGCAGGAA;

Cxcr7: CAAACCACAGCCCAGGAA, CATGGCCAGTTGATGTCAGA;

Pgk1: GCGCTGTTCTCCTCTTCCTC, GTCCACCCTCATCACGACC;

Cxcl12: CTGCATCAGTGACGGTAAACC, TCTTCAGCCGTGCAACAATC.

Image Acquisitions and Processing. Image acquisitions were done using the ApoTome optical sectioning system (Zeiss) with an inverted microscope (Zeiss Axio Observer Z1) for immunofluorescent images and with a Nikon microscope (type 120c) for chromogenic images. All quantifications were performed without knowing the corresponding genotypes. ImageJ and Adobe Photoshop and Illustrator were used for image processing in compliance with the journal's guidelines for digital image processing. For fluorescence images, ImageJ background subtraction was performed identically on all pictures using a rolling ball radius of 50 pixels. When several groups of images were compared, contrast and brightness were adjusted identically on all images. For histomorphometry, quantifications were done using Bonolab software (Microvision Instruments). All other quantifications were performed using ImageJ and Icy.

Statistics. For all graphics, data are presented as mean ± SEM. Dot plots represent biological replicates. The sample size number (*n*) represents independent mice for in vivo experiments and

independent cell isolations for in vitro experiments. Sample size estimations were calculated to obtain a power of at least 80% and were based on the initial size effect obtained with preliminary experiments, which included a minimum of three mice for each group analyzed. Of note, we did not work with a fixed number of mice, since all animals included in our experiments are control and conditional knockout littermates, whose numbers are variable in each litter. For Kaplan–Meier survival curves, log-rank (Mantel–Cox) tests were performed to compare curves. When comparing the effect of a treatment or different breast cancer cell lines on control and mutant mice, two-way ANOVA was used with Bonferroni posttests. In other panels, statistical analysis was performed using unpaired two-sided Student's t test. Resulting P values are represented as follows: $^{*}P < 0.05$; $^{**}P < 0.01$; $^{***}P < 0.001$; $^{****}P < 0.0001$. All statistical analyses were performed using GraphPad Prism software (version 5.0f).

1. Gruber M, et al. (2007) Acute postnatal ablation of Hif-2alpha results in anemia. *Proc Natl Acad Sci USA* 104:2301–2306.
2. Haase VH, Glickman JN, Socolovsky M, Jaenisch R (2001) Vascular tumors in livers with targeted inactivation of the von Hippel-Lindau tumor suppressor. *Proc Natl Acad Sci USA* 98:1583–1588.
3. Rodda SJ, McMahon AP (2006) Distinct roles for hedgehog and canonical Wnt signaling in specification, differentiation and maintenance of osteoblast progenitors. *Development* 133:3231–3244.
4. Ryan HE, Lo J, Johnson RS (1998) HIF-1 alpha is required for solid tumor formation and embryonic vascularization. *EMBO J* 17:3005–3015.
5. Lin EY, et al. (2003) Progression to malignancy in the polyoma middle T oncoprotein mouse breast cancer model provides a reliable model for human diseases. *Am J Pathol* 163:2113–2126.
6. Reilly RT, et al. (2000) HER-2/neu is a tumor rejection target in tolerized HER-2/neu transgenic mice. *Cancer Res* 60:3569–3576.
7. Zhu H, et al. (2010) A protocol for isolation and culture of mesenchymal stem cells from mouse compact bone. *Nat Protoc* 5:550–560.
8. Passaro D, et al. (2015) CXCR4 is required for leukemia-initiating cell activity in T cell acute lymphoblastic leukemia. *Cancer Cell* 27:769–779.
9. Arguello F, Baggs RB, Frantz CN (1988) A murine model of experimental metastasis to bone and bone marrow. *Cancer Res* 48:6876–6881.
10. Kocatürk B, Versteeg HH (2015) Orthotopic injection of breast cancer cells into the mammary fat pad of mice to study tumor growth. *J Vis Exp* 96:e51967.
11. Parfitt AM, et al. (1987) Bone histomorphometry: Standardization of nomenclature, symbols, and units. Report of the ASBMR Histomorphometry Nomenclature Committee. *J Bone Miner Res* 2:595–610.
12. Kusumbe AP, Ramasamy SK, Adams RH (2014) Coupling of angiogenesis and osteogenesis by a specific vessel subtype in bone. *Nature* 507:323–328.
13. Schepers K, et al. (2013) Myeloproliferative neoplasia remodels the endosteal bone marrow niche into a self-reinforcing leukemic niche. *Cell Stem Cell* 13:285–299.

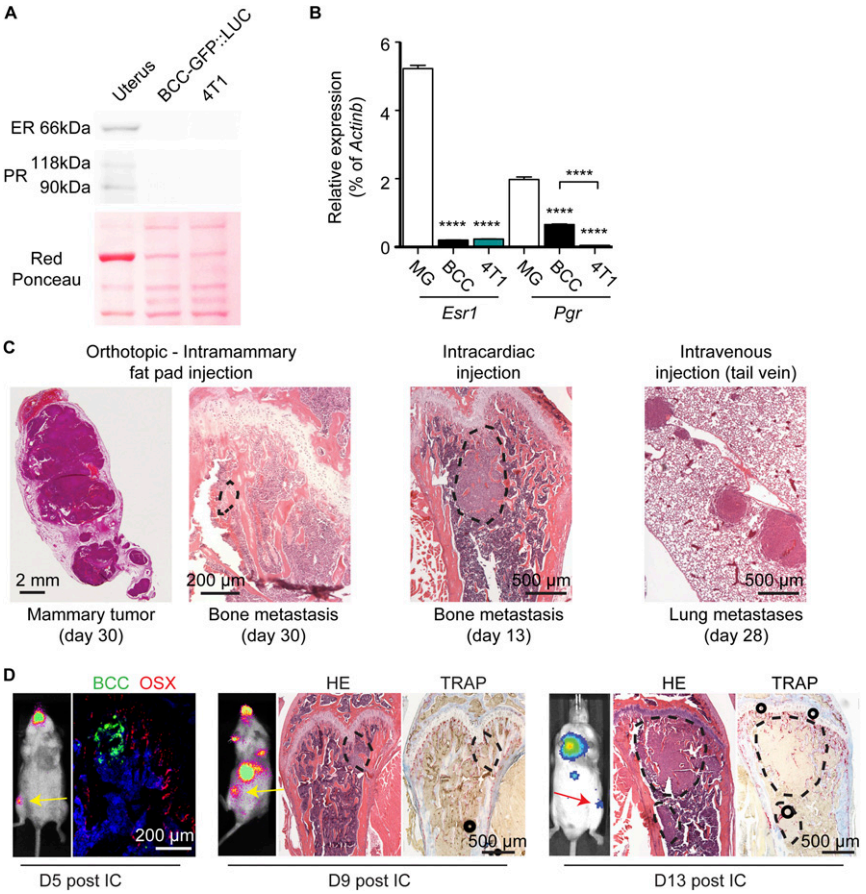

Fig. S1. The breast cancer cell line BCC-GFP::LUC has low ER-PR expression and generates osteolytic bone metastases. (*A*) Western blot analysis for ER and PR. Ponceau red coloration is used to verify even loading. Protein lysates of mouse uterus and the 4T1 triple-negative murine breast cancer cell line are used as positive and negative controls, respectively. (*B*) Hormone receptor status analyzed by mRNA expression (qPCR) of *Esr1* (ER) and *Pgr* (PR) expressed as percentage of the expression of the reference gene *Actinb*. Mammary gland (MG) is used as positive control ($n = 3$). Values indicate the mean ± SEM; $^{*}P < 0.05$, $^{**}P < 0.01$, $^{***}P < 0.001$, $^{****}P < 0.0001$; two-tailed Student's t test. (*C*) Examples of mammary tumors obtained after i.f.p. transplantation, bone metastases obtained after i.c. injection, and lung metastases obtained after i.v. injection. (*D*) Bioluminescence images and histological analyses of hind limbs 5, 9, and 14 d after i.c. injection of 10,000 BCC-GFP::Luc cells. Metastases that were histologically analyzed are indicated by arrows in the whole-animal images and are circled with dashed lines on the histology images. (*Left*) BCC-GFP::Luc cells are stained in green for GFP, and OPCs are stained in red for OSX expression. (*Right*) TRAP staining detects osteoclasts in red. HE, H&E staining.

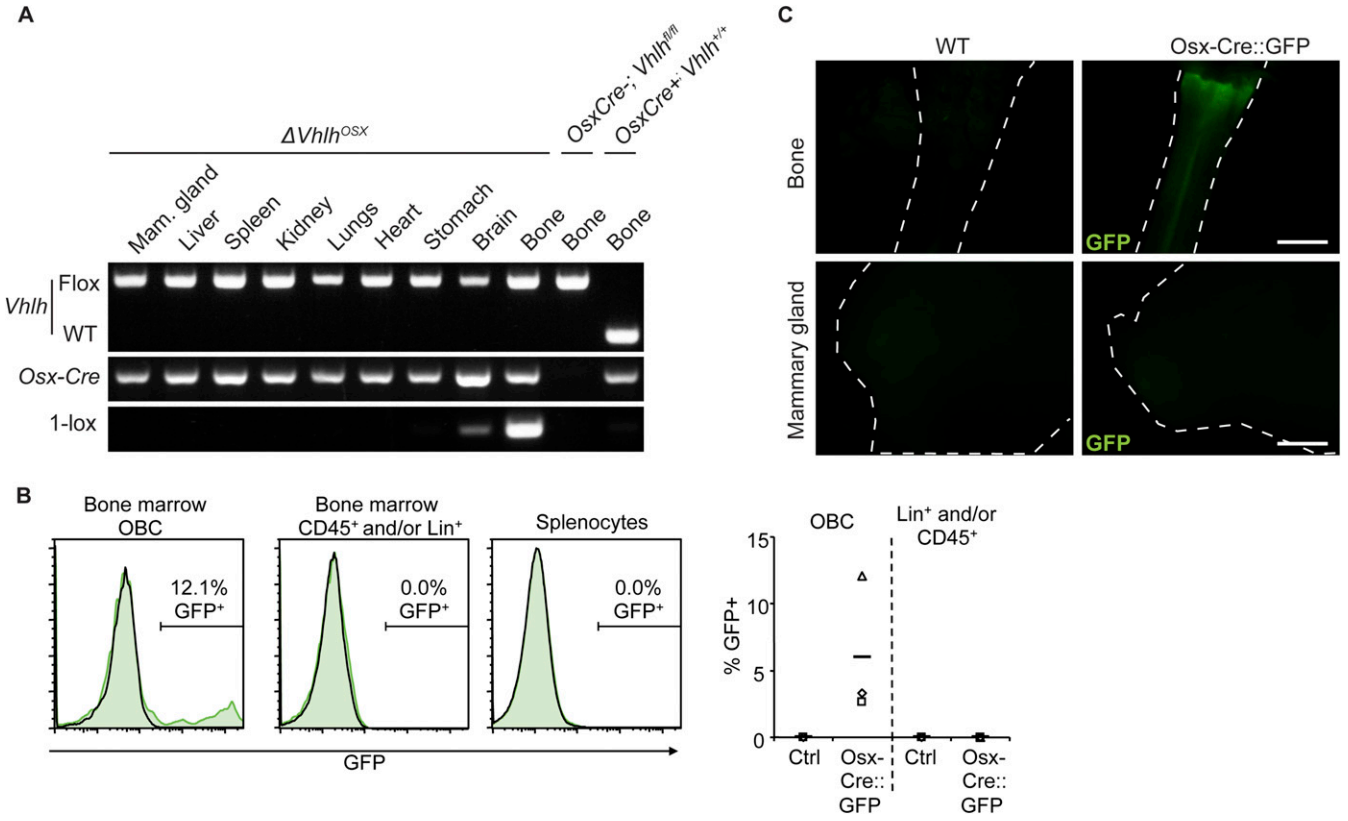

Fig. S2. Specificity of Osx-Cre::GFP–induced recombination. (*A*) Genomic PCR analysis for the *Cre*, *Vhlh* floxed allele, and *Vhlh* recombined allele (1-lox) of genomic DNA isolated from $\Delta Vhlh^{OSX}$ and controls [Cre^- and *Vhlh* floxed homozygous tissues or Cre^+ tissues without the floxed allele (WT)]. (*B*) FACS analysis of the bone marrow and the spleen isolated from Osx-Cre::GFP transgenic mice, showing the presence of GFP^+ cells only in the pool of Lin^- $CD45^-$ $CD31^-$ $CD51^+$ $Sca1^-$ osteoblast lineage-cells (OBC) but not in the pool of $CD45^+$ or Lin^+ hematopoietic cells and not in the spleen. (*C*) Detection of GFP expression (in green) in femurs and mammary glands of wild-type and Osx-Cre::GFP transgenic animals. Some weak autofluorescence is observed in wild-type mammary glands. (Scale bars: 1,320 μm.)

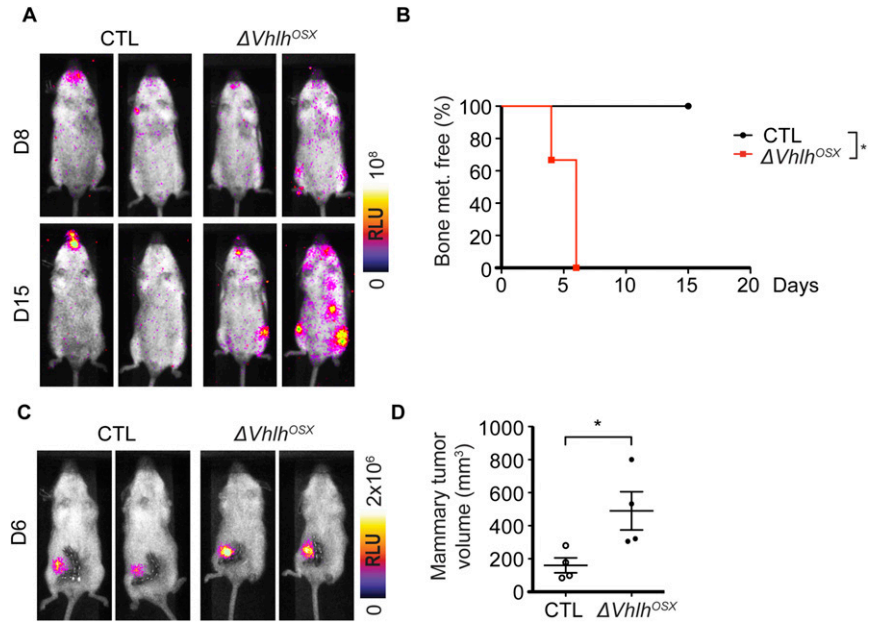

Fig. S3. HIF signaling in the osteoblast lineage promotes systemic breast cancer growth and dissemination of NT2.5 breast cancer cells. (*A* and *B*) Representative bioluminescent images (*A*) and Kaplan–Meier analysis (*B*) of bone metastasis after i.c. injection of NT2.5 breast cancer cells in control ($n = 3$) and $\Delta Vhlh^{OSX}$ mice ($n = 3$). (*C* and *D*) Representative bioluminescent images (*C*) and quantification of tumor volumes (*D*) obtained after i.f.p. transplantation of NT2.5 cells in control ($n = 4$) and $\Delta Vhlh^{OSX}$ ($n = 4$) mice. Values indicate the mean ± SEM; $^*P < 0.05$; log-rank (Mantel–Cox) test (*B*) or two-tailed Student's *t* test (*D*).

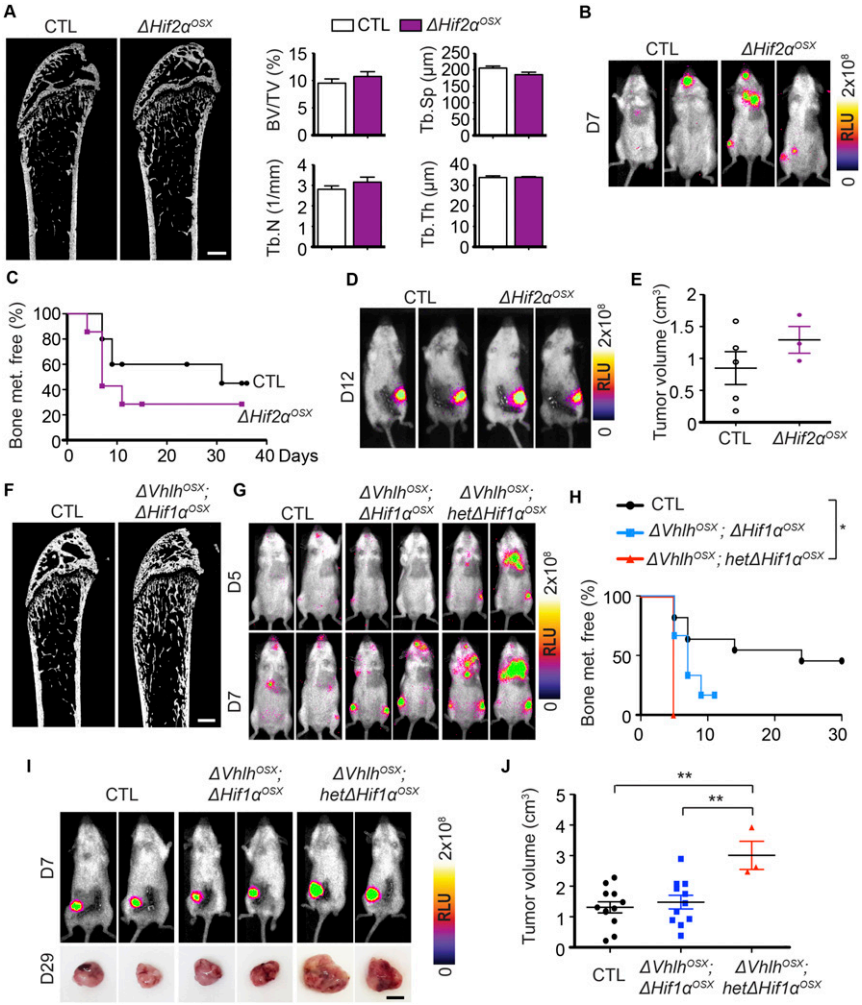

Fig. S4. Osteoblast-lineage cells promote breast cancer growth and dissemination through HIF1α. (*A*) Representative micro-CT images of femurs and 3D analyses of BV/TV, Tb.N, Tb.Sp, and Tb.Th of 8-wk-old control and $\Delta Hif2\alpha^{OSX}$ male mice ($n = 3$). (*B* and *C*) Representative bioluminescent images (*B*) and Kaplan–Meier analysis (*C*) of bone metastasis obtained after i.c. injections of BCC-GFP::LUC cells in control ($n = 10$) and $\Delta Hif2\alpha^{OSX}$ ($n = 7$) mice. (*D* and *E*) Representative bioluminescent images (*D*) and quantification of tumor volumes (*E*) obtained after i.f.p. transplantation of BCC-GFP::LUC in control ($n = 5$) and $\Delta Hif2\alpha^{OSX}$ ($n = 3$) mice. (*F*) Representative micro-CT images of femurs of 8-wk-old control and $\Delta Vhlh^{OSX}; \Delta Hif1\alpha^{OSX}$ double-conditional-knockout mice. (*G* and *H*) Representative bioluminescent images (*G*) and Kaplan–Meier analysis (*H*) of bone metastasis obtained after i.c. injections of BCC-GFP::LUC cells in control ($n = 11$), $\Delta Vhlh^{OSX}; \Delta Hif1\alpha^{OSX}$ ($n = 6$), and $\Delta Vhlh^{OSX}; het\Delta Hif1\alpha^{OSX}$ ($n = 3$) mice. (*I* and *J*) Representative bioluminescent images and tumor photographs (*I*) and quantifications of tumor volumes (*J*) obtained 29 d after i.f.p. transplantation of BCC-GFP::LUC cells in control ($n = 12$), $\Delta Vhlh^{OSX}; \Delta Hif1\alpha^{OSX}$ ($n = 11$), and $\Delta Vhlh^{OSX}; het\Delta Hif1\alpha^{OSX}$ ($n = 3$) mice. (Scale bars: 500 μm in *A* and *F*; 1 mm in *I*.) Values indicate the mean ± SEM. $^*P < 0.05$, $^{**}P < 0.01$; log-rank (Mantel–Cox) test (*C* and *H*), two-tailed Student's *t* test (*E* and *J*).

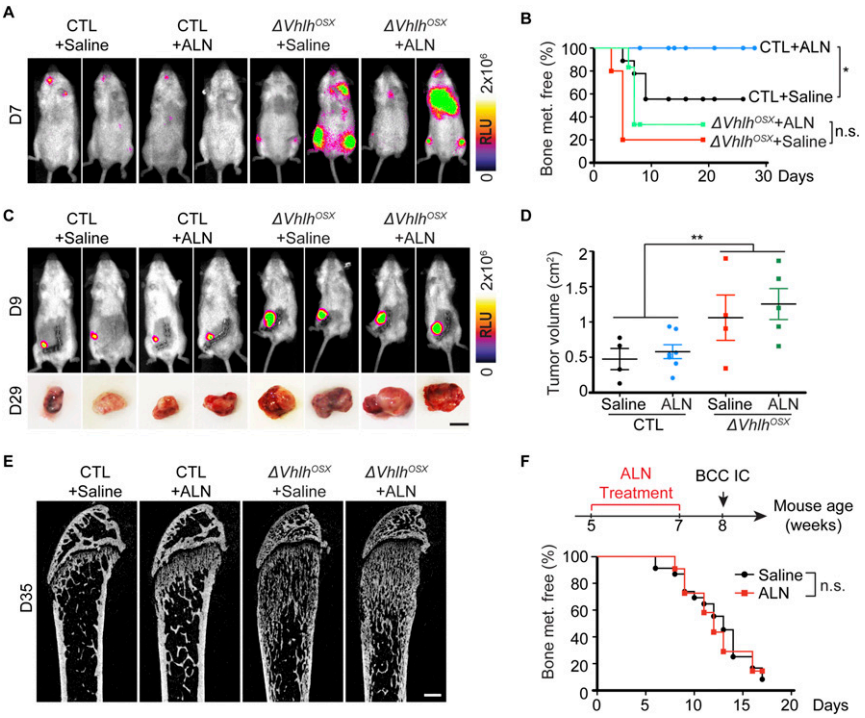

Fig. S5. Osteoclasts do not mediate systemic breast cancer growth and dissemination in $\Delta Vhlh^{OSX}$ mice. (*A* and *B*) Representative bioluminescent images (*A*) and Kaplan–Meier analysis (*B*) of bone metastasis after i.c. injections of BCC-GFP::LUC cells in control mice treated with saline ($n = 9$) or ALN ($n = 10$) and in $\Delta Vhlh^{OSX}$ mice ($n = 5$ for saline and $n = 6$ for ALN). (*C* and *D*) Representative bioluminescent images (*C*) and tumor photographs and quantification of tumor volumes (*D*) 29 d after i.f.p. transplantation of BCC-GFP::LUC cells in control mice ($n = 4$ for saline and $n = 7$ for ALN) and $\Delta Vhlh^{OSX}$ mice ($n = 4$ for saline and $n = 5$ for ALN). Two-way ANOVA revealed no significant (n.s.) effect of ALN treatments. (*E*) Representative micro-CT images of femurs of control and $\Delta Vhlh^{OSX}$ mice treated for 5 wk with saline or ALN (an inhibitor of osteoclast activity) showing increased trabecular bone volume. (*F*) Kaplan–Meier analysis of bone metastasis after i.c. injections of BCC-GFP::LUC cells in wild-type mice pretreated with saline ($n = 12$) or ALN ($n = 11$) for 2 wk before i.c. injections. (Scale bars: 1 cm in *C* and 500 μm in *E*.) Values indicate the mean ± SEM; $^*P < 0.05$, $^{**}P < 0.01$; log-rank (Mantel–Cox) test (*B* and *F*) or two-way ANOVA (*D*).

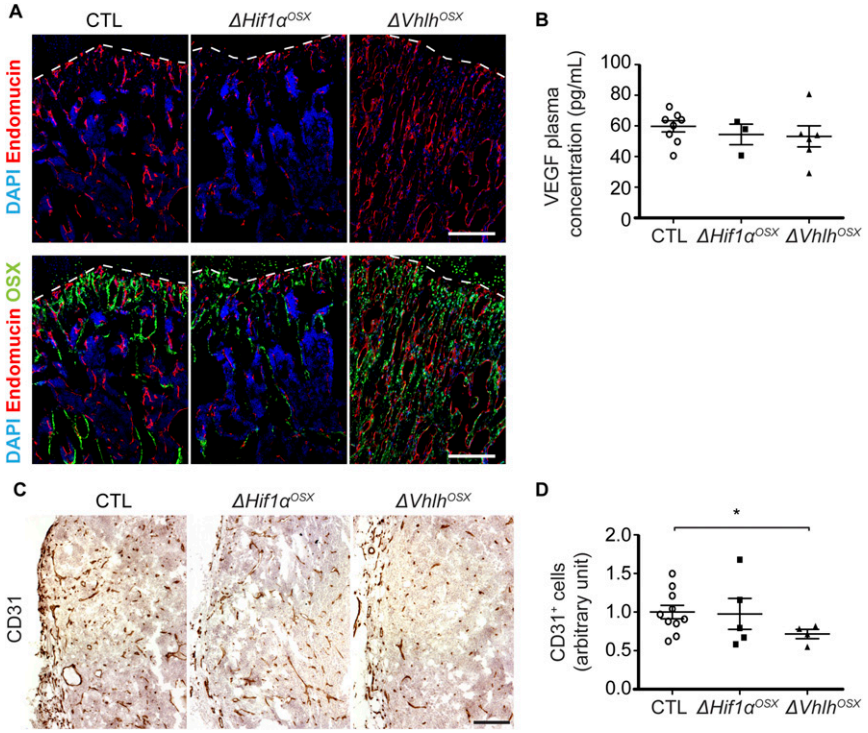

Fig. S6. Activation of HIF signaling in osteoblast-lineage cells does not increase angiogenesis outside the skeleton. (*A*) Immunostaining against the endothelial cell marker Endomucin (in red) and OSX$^+$ OPCs (in green) in hind limbs of 8-wk-old mice. Dashed lines indicate the limit between cartilage (above the dashed line) and bone (below the dashed line). (*B*) ELISA showing plasma VEGF levels (expressed in picograms per milliliter) in control ($n = 8$), $\Delta Hif1\alpha^{OSX}$ ($n = 3$), and $\Delta Vhlh^{OSX}$ ($n = 6$) mice. (*C* and *D*) Representative photographs (*C*) and quantification (*D*) of cells positive for the endothelial cell marker CD31 by immunostaining of mammary tumors harvested 12 d after i.f.p. transplantation of BCC-GFP::LUC cells in control ($n = 10$), $\Delta Hif1\alpha^{OSX}$ ($n = 5$), and $\Delta Vhlh^{OSX}$ ($n = 4$) mice. The number of cells detected per tissue area was normalized to average control. (Scale bars: 200 μm.) Values indicate the mean ± SEM; $^*P < 0.05$; two-tailed Student's *t* test.

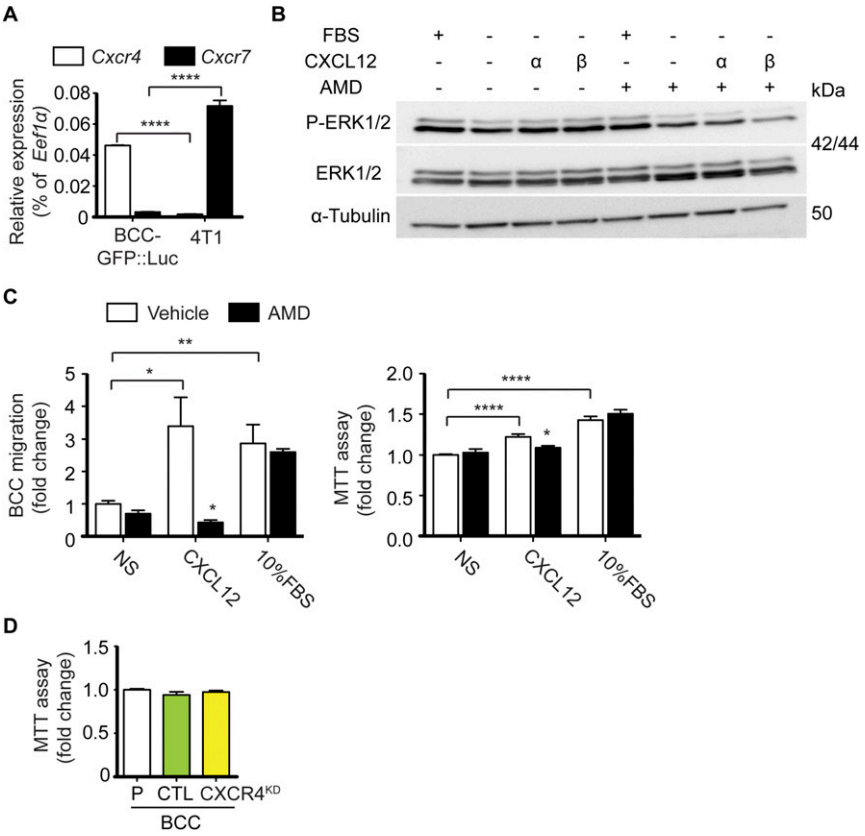

Fig. S7. CXCL12 activates BCC-GFP::LUC through CXCR4. (*A*) Relative mRNA expression of *Cxcr4* and *Cxcr7* in murine breast cancer cell lines 4T1 and BCC-GFP::LUC ($n = 3$). (*B*) Western blot of phospho-ERK1/2, total ERK1/2, and tubulin on BCC-GFP::LUC cells stimulated with 10% FBS and CXCL12 α or β isoforms and treated (+) or not treated (–) with AMD3100. (*C*, *Left*) Migration assay of BCC-GFP::LUC cells. (*Right*) MTT assay measuring the proliferation of BCC-GFP::LUC cells either not stimulated (NS; serum-free medium) or stimulated with recombinant CXCL12 or with 10% FBS in the presence or absence of AMD3100. Values ($n \geq 4$) are normalized to nonstimulated controls. (*D*) MTT assay indicating the proliferation of parental BCC-GFP::LUC cells (P), or BCC-GFP::LUC cells transduced with control lentiviruses (BCC-CTL) or with lentiviruses expressing shRNA against *Cxcr4* (BCC-CXCR4^{KD}) ($n \geq 4$). Values indicate the mean ± SEM; $^{*}P < 0.05$, $^{**}P < 0.01$, $^{****}P < 0.0001$; two-tailed Student's *t* test.

Table S1. Primary antibodies and antigen retrieval methods

Primary antibody	Antigen retrieval	Dilution
FITC anti-GFP (ab6662; Abcam)	0.3% Triton X-100 10 min	1:500
Anti-HIF1α (ab2185; Abcam)	0.3% Triton X-100 10 min	1:100
Anti-HIF2α (NB100-122; Novus)	0.3% Triton X-100 10 min	1:100
Anti-OSX (sc-22536R; Santa Cruz)	0.3% Triton X-100 10 min	1:200
Anti–phospho-histone H3 (9701; Cell Signaling Technology)	0.3% Triton X-100 10 min	1:400
Anti-CXCL12 (14-7992; eBioscience)	1% H_2O_2 30 min	1:100
Anti-CD31 (DIA-310; Dianova)	0.5% Tween20 10 min	1:100
Anti-endomucin (sc65495; Santa Cruz)	0.3% Triton X-100 10 min	1:200